And., Intl.,J., Appl Sci., Eng., Tech, Vol 04, No 02, July 2024
e-ISSN: 2797-0442

Design of Multi-Level Inverter Design for Charging Stations of Electric Vehicles

Aung Kyaw Htay[1], Hla Myo Tun[2*], Devasis Pradhan[3], Lei Lei Yin Win[1], Ei Ei Khin[1], Khaing Thandar Soe[1]
[1]Department of Electronic Engineering, Yangon Technological University, Myanmar.
[2]Research Department, Yangon Technological University, Myanmar.
[3]Department of ECE, Acharya Institute of Technology, India.
[*]Corresponding author, e-mail: hmt.ytu@gmail.com

Abstract— The paper mainly focuses on the Design of Multi-Level Inverter Design for Charging Stations of Electric Vehicles. The research challenges in this study are: the lack of technology for higher level design of multilevel inverter systems for electric vehicles (EVs) is facing to solve the high performance and robustness of the system in reality, the control algorithm for maximum power observing is a crucial challenge in the designing and implementing such kind of multilevel inverter design, the pure sine wave inverter approaches with higher number steps could be a candidate for electric vehicles (EVs) in real world applications. That problems could be solved based on the knowledge and idea of power electronic circuits and systems. The implementation of this study was accomplished based on the specific model especially based on the circuit theory and microelectronic devices. The results confirm that the performance specification of targeted multilevel inverter (MLI) in real world applications.

Keywords: Multi Level Inverter; Converter Design; Power Electronics; Renewable Energy Sources, Electric Vehicles.

1. Introduction

The With the demand for an increase in the requirements of high-power quality in industrial applications and solar PV systems, the conventional inverters in meeting the desired conditions like a pure sine-wave output and less harmonic distortions is a challenging task. The multilevel inverters receive more attention in reaching the desired requirements and acts as an alternative in delivering a quality of power. The number of components in the circuit is directly proportional to the number of levels in MLI, which increases cost and complex structure. A wide range of research is reducing the components of MLI, and several topologies are proposed based on the various levels which are having their challenges [1-6].

The lack of technology for higher level design of multilevel inverter systems for electric vehicles (EVs) is facing to solve the high performance and robustness of the system in reality. The control algorithm for maximum power observing is a crucial challenge in the designing and implementing such kind of multilevel inverter design. The pure sine wave inverter approaches with higher number steps could be a candidate for electric vehicles (EVs) in real world applications. That problems could be solved based on the knowledge and idea of power electronic circuits and systems. [7-10]

Received: June 24, 2024, Revised: 10 July, 2024, Accepted: 16 July, 2024
https://doi.org/ 10.25077/aijaset.v4i2.136

AIJASET – Vol. 04, No. 02, July 2024. 125-136
https://doi.org/ 10.25077/aijaset.v4i2.136

The research objectives are as follows:
(1) To model the mathematical analysis on proposed inverter design
(2) To implement the SIMULINK model for confirmation of the numerical analysis
(3) To design the developed model in SIMULINK with hardware elements
(4) To measure the physical characteristics of the implemented inverter systems
(5) To evaluate the performance of the developed system
The research methodologies are based on the following ideas.
(1) Study on semiconductor power electronic devices for high power applications.
(2) Design and construct of basic inverter systems with specific circuit models.
(3) Analyze the mathematical model for those inverter systems and developing the SIMULINK model.
(4) Modelling and constructing of the novel design for efficient purposes for designing the converter systems in EV fast charging station.
(5) Performance evaluating of the developed conditions.

2. Overall Circuit Diagram and Results

The DC to DC booster will take part in this system as the voltage booster for the main system which is the 15-level multilevel inverter. DC-DC booster steps up the source input voltage and regulate its average output voltage larger than the source voltage. The regulator in this DC-DC booster will be a 7809 voltage regulator. Moreover, the energy will be storing enough in the inductor so that the output is the desired voltage throughout the switching action. The switch will be power MOSFET IRF540 because of the reason that it can simplify the control of the booster. The output voltage is also manipulated by Power Schottky Rectifier because of its negligible switching losses and extremely fast switching abilities. The average output voltage, VO is controlled by the duty cycle of the switch which in turn is controlled by the PWM controller UC3842. Finally, the desired boosted output voltage 48V for multilevel inverter will be obtained. Figure 1 shows the circuit diagram of DC-DC Converter. Figure 2 illustrates the MOSFET Switching Circuit.

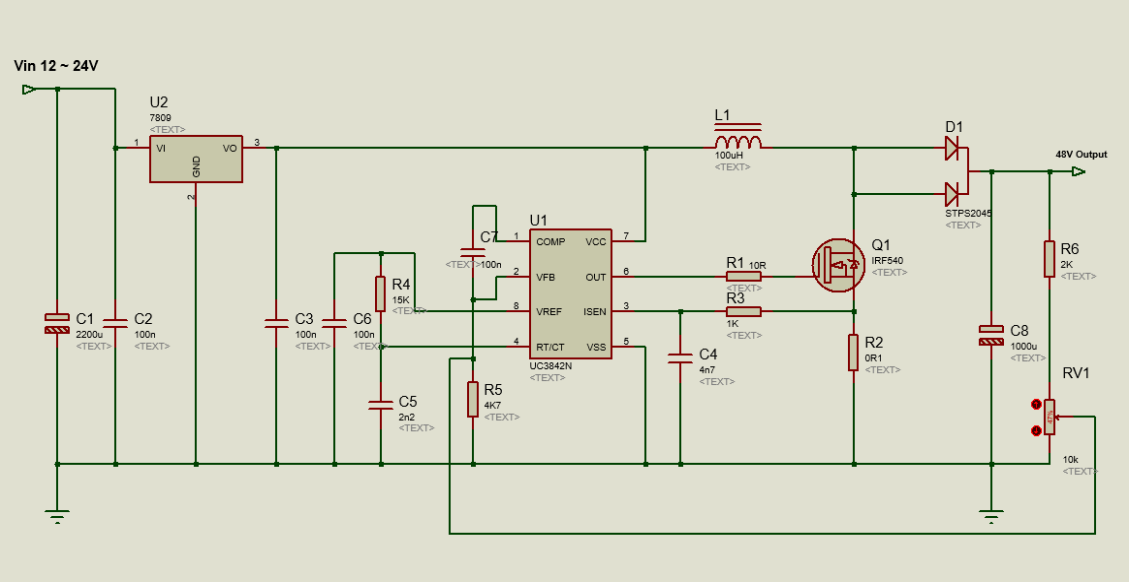

Figure 1. DC-DC Converter

2.1 Detailed Calculations for Oscillator Timing Capacitor

Oscillator Frequency, $f_{OSC} = \frac{1.72}{R_T \times C_T}$ (1)

Where R_T = oscillator timing resistor

C_T = oscillator timing capacitor

Select f_{OSC} = 50kHz, C_T = 2.2 nF,

$50k = \frac{1.72}{R_T \times 2.2n}$

R_T = 15.6kΩ

R_4 = 15kΩ

Therefore, R_4 = 15kΩ is chosen as the standard resistor value.

2.2. Detailed Calculations for Inductor

Cutoff frequency, $f = \frac{1}{2\pi\sqrt{LC}}$ (2)

Select f = 500Hz which is the cutoff from $f_{OSC,}$

C = 1000µF selected from $C_{8,}$

$500 = \frac{1}{2\pi\sqrt{L} \times 1000\mu}$

L = 101µF

Therefore, L = 100µF is selected which is the standard value.

2.3. Design Calculation of Gate Resistor of MOSFET

From specifications of UC3842N,

OUTPUT voltage, V = 10V

Maximum Peak current, I = 1A

Gate resistor, $R_G = \frac{10}{1} = 10\Omega$

Therefore, R_1 is selected as 10Ω.

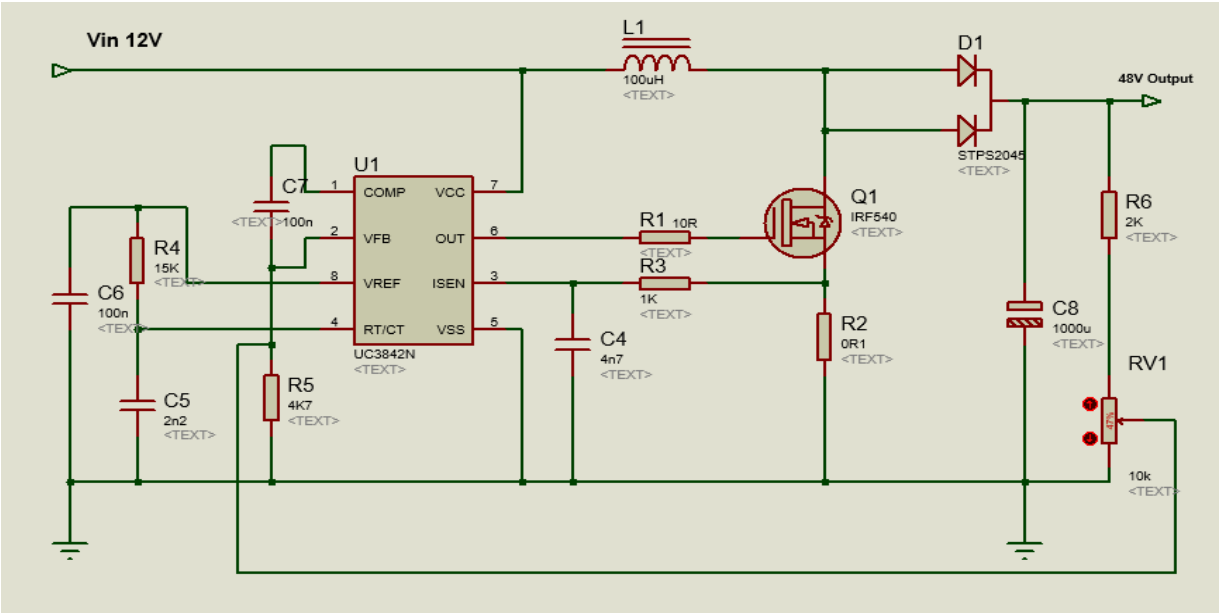

Figure 2. MOSFET Switching Circuit

2.4. Circuit Diagram of Simulation of DC-DC Booster Design

The oscilloscope is connected to the PWM controller, UC3842N and simulated the output wave from it. Figure 3 demonstrates the Simulation Diagram for DC-DC Converter.

AIJASET – Vol. 04, No. 02, July 2024. 125-136
https://doi.org/ 10.25077/aijaset.v4i2.136

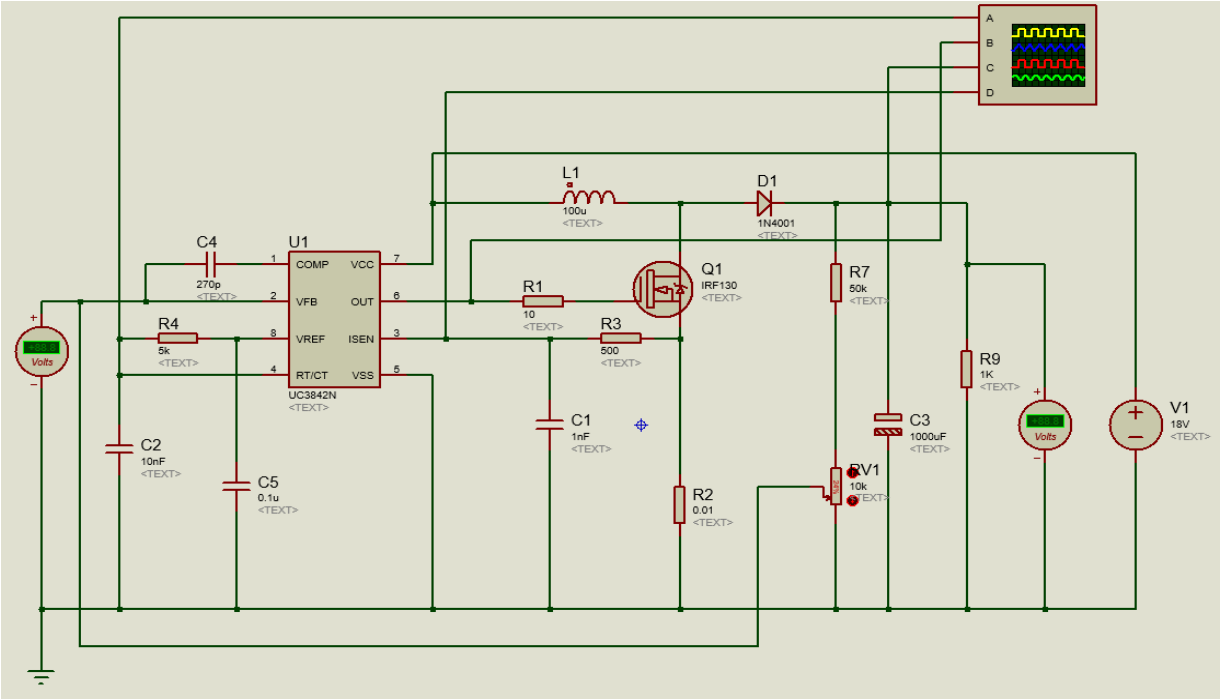

Figure 3. Simulation Diagram for DC-DC Converter

2.5. Design Calculation of Multilevel Power Source Battery Bank Circuit

The obtained 48V from DC-DC booster is treated as a overall input voltage which is divided into 8 cells in order to obtain 15 steps. Therefore, an individual input voltage for each cell becomes 6V. High density mounting type photocoupler which PC817 is used in the circuit because of its high isolation voltage between input and output. As for the MOSFET, IRF9540N is chosen because of its features such as fast switching speed and fully avalanched rated. By combining them, they perform as cascaded multiple MOSFET array. Figure 4 mentions the Circuit Diagram for DC Sources.

2.6. Design Calculation of H-Bridge Inverter

The H-bridge inverter is used to switch the polarity of a voltage applied to a load. It is built with four switches in which include PC817 optocouplers and IRF540 MOSFETs. The operation of the H-bridge inverters is that when U12 and U10 are opened while U9 and U11 closing which is vice versa. Multilevel output can be detected from each side of the H-bridge inverter unit. 12V input is provided for each switch. Figure 5 shows the H-Bridge Inverter.

2.7. Design Calculation of the Gate Resistor of MOSFETs

For the upper side of H-bridge inverter,

$$R = \frac{V_{CC} - V_{drop} - V_{CE}}{I_C} \quad (3)$$

Selecting required values from the specifications of IRF540 MOSFET,

$$R = \frac{12 - 1.7 - 6}{50m}$$

$R = 86\Omega$

Therefore, R_9 and R_{11} are chosen as 100Ω which is a standard value.

For the lower side of H-bridge Inverter,

R= (V_CC-V_CE)/I_C

Selecting required values from the specifications of IRF540 MOSFET,

R= (12-6)/50m

R = 120Ω

Therefore, R13 and R15 are chosen as 100Ω as standard value. Figure 6 illustrates the Gate Resistor Design.

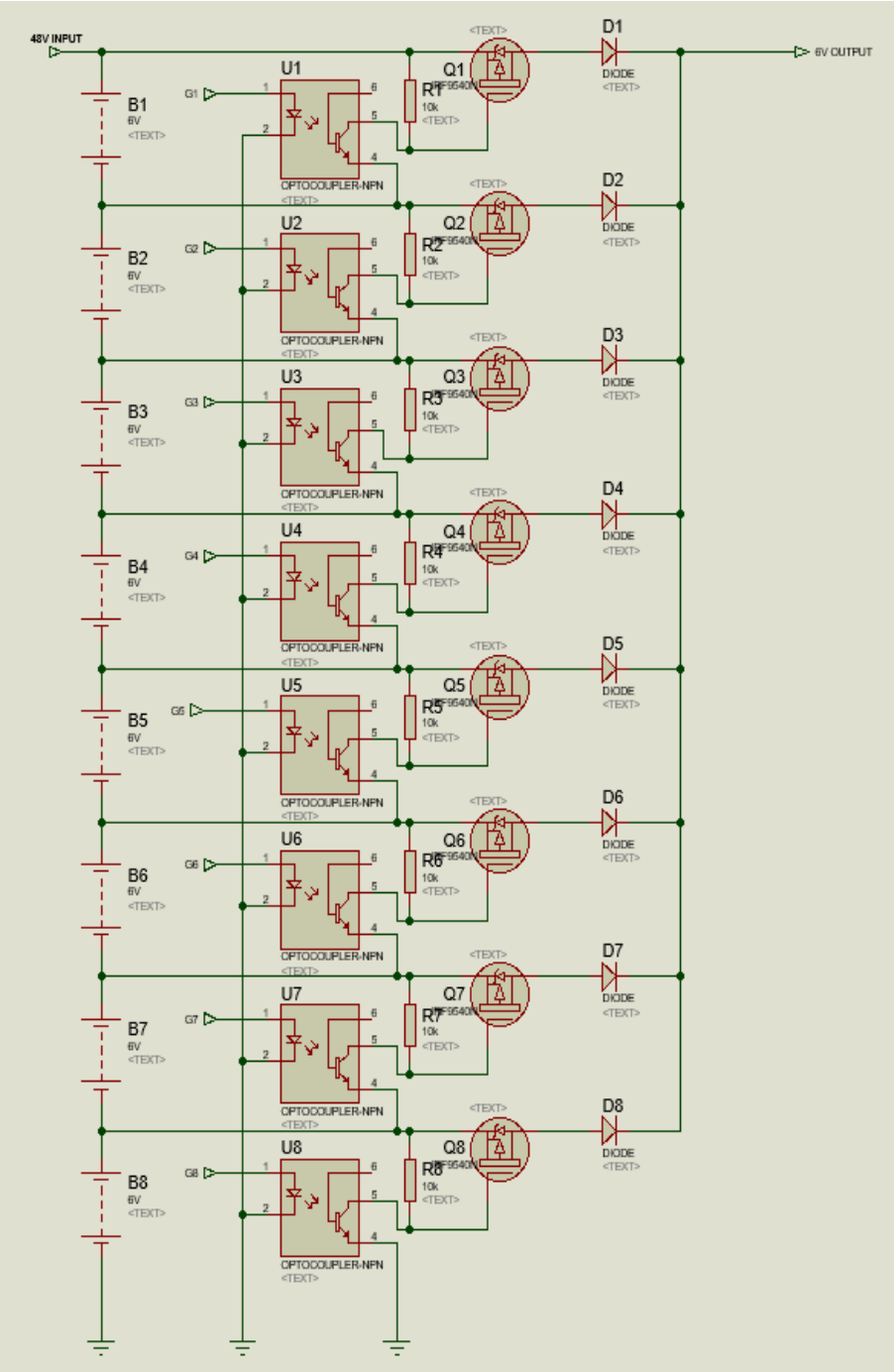

Figure 4. Circuit Diagram for DC Sources

2.8. Design Calculation for Bootstrap Capacitance

$$C_{min} \geq \frac{2[2Q_g + \frac{I_{qbs(max)}}{f} + Q_{ls} + \frac{I_{cbs}}{f}]}{V_{CC} - V_f - V_{LS} - V_{min}} \quad (4)$$

where, Q_g = Gate charge of high-side FET
f = Frequency of operation
I_{cbs} = Boostrap capacitor leakage current

AIJASET – Vol. 04, No. 02, July 2024. 125-136
https://doi.org/ 10.25077/aijaset.v4i2.136

I_{qbs} = Maximum quiescent current
Q_{ls} = Level shift charge required per cycle
V_{CC} = Logic section voltage source
V_f = Forward voltage drop across the bootstrap diode
V_{LS} = Voltage drop across the low-side FET or load
V_{min} = Minimum voltage on the bootstrap capacitor

Selecting required values from the specifications of IRF540 MOSFET,
Assume V_{min} = 7.5V (2V < V_{GS} < 20V)

$$C_{min} \geq \frac{2[2 \times 65n + \frac{230\mu}{50k} + 5n + \frac{250\mu}{50k}]}{12 - 1.7 - 1.5 - 7.5}$$

$$C_{min} \geq 0.22\mu F$$

Therefore, bootstrap capacitance value is chosen as 47µF which is standard, just above the calculated value and enough for the MOSFETs. Figure 7 demonstrates the Optocoupler Circuit Connection.

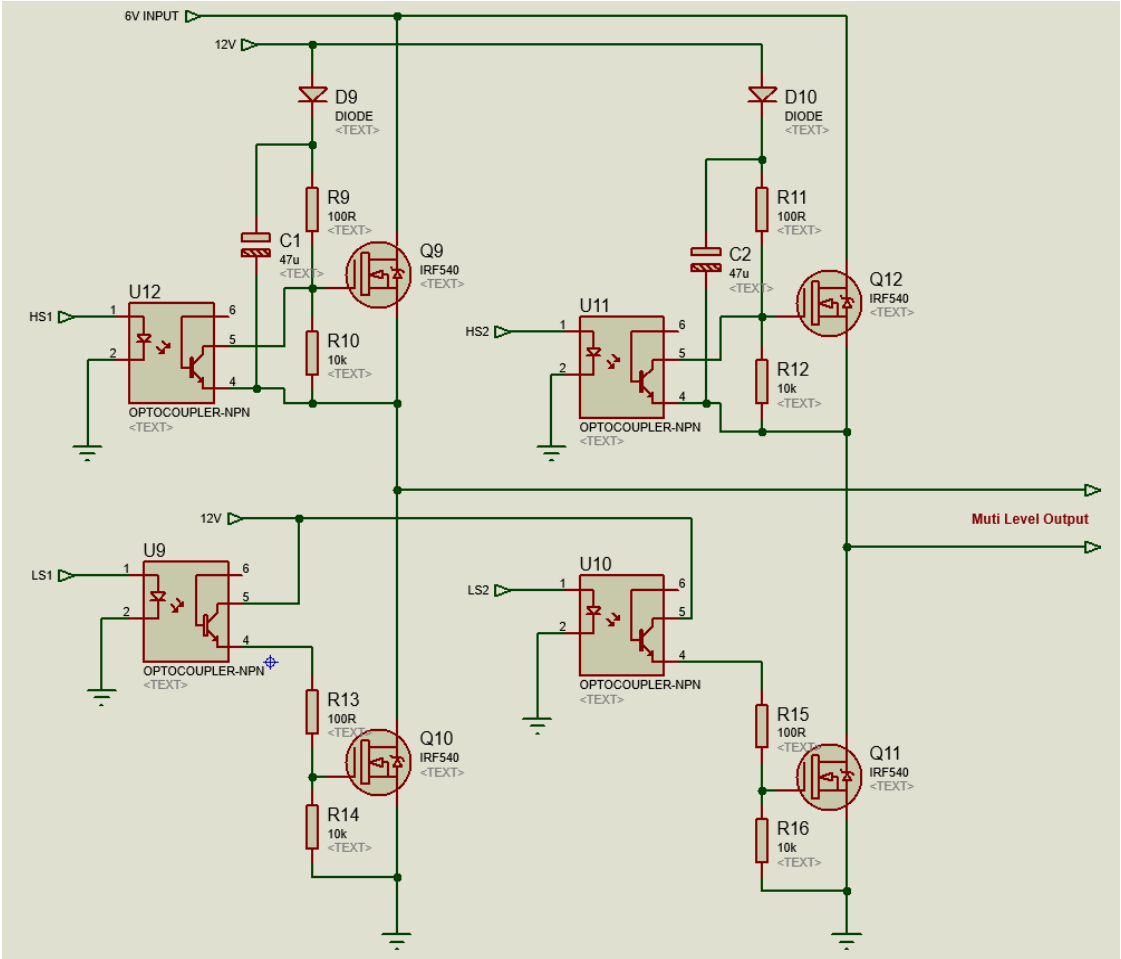

Figure 5. H-Bridge Inverter

2.9. Design Calculation and Software Implementation of PIC Controller

Figure.8 shows the PIC controller circuit which controls the switching steps of the H-bridge multilevel inverter. First of all, the input 5V is given and then regulated by 78L05 positive voltage regulator. A controller used in the circuit is PIC 16F667 microcontroller with 20 pins because of its high-performance and efficient features. Figure 8 illustrates the PIC Controller Connection Design.

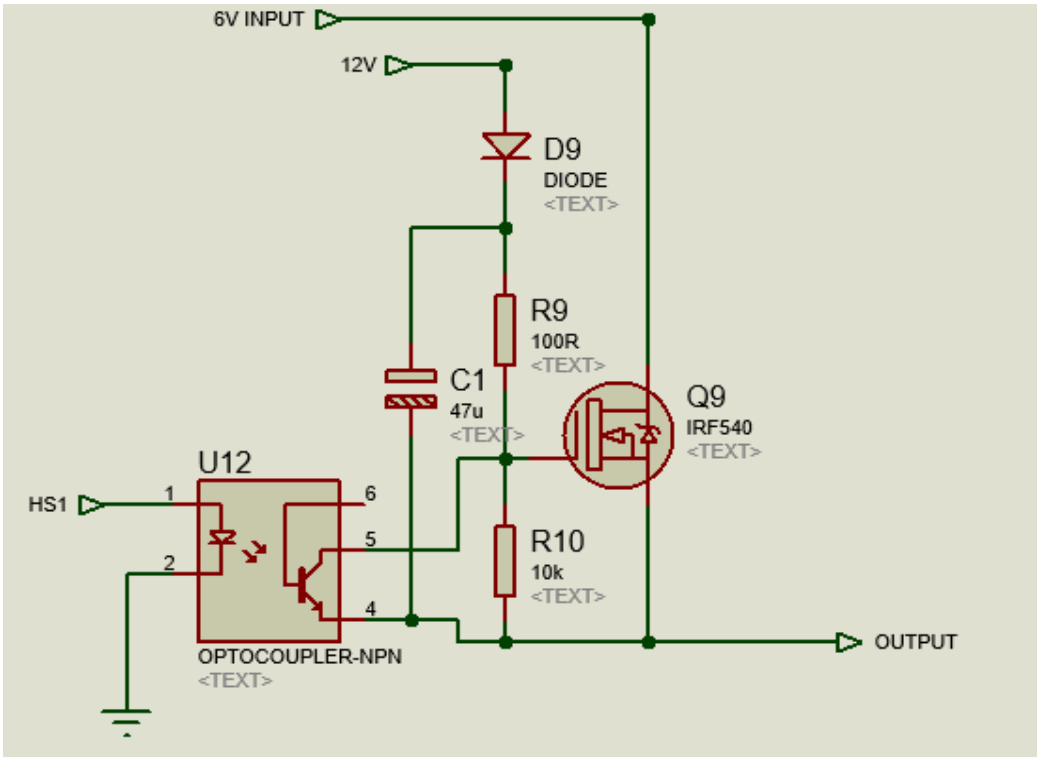

Figure 6. Gate Resistor Design

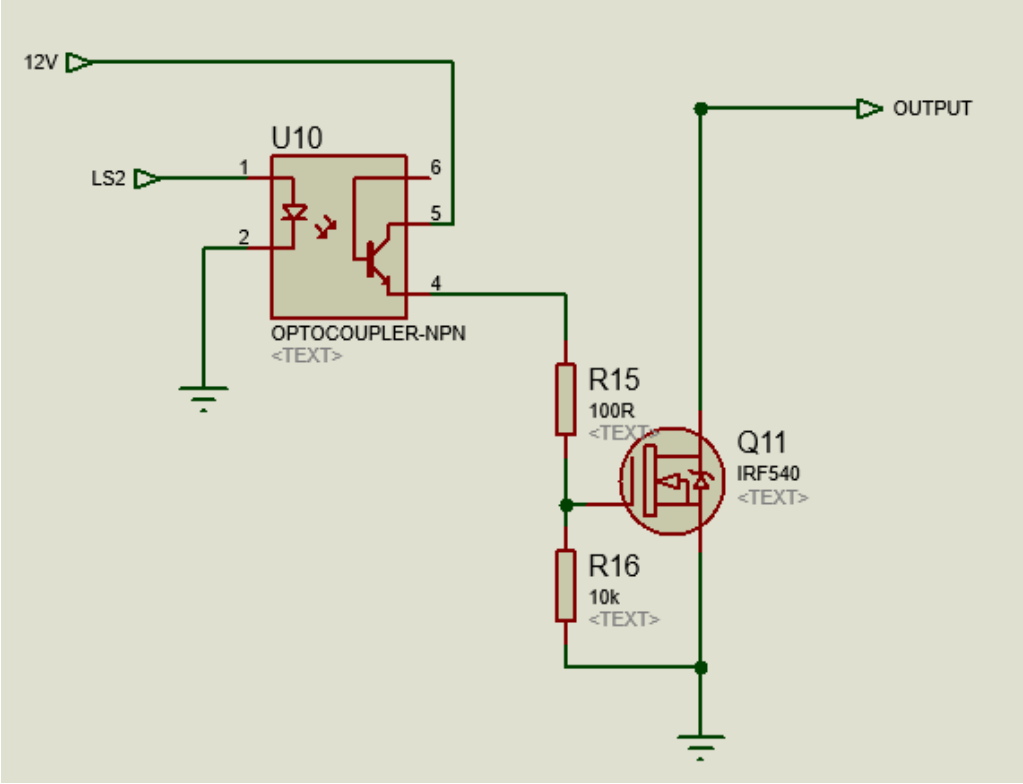

Figure 7. Optocoupler Circuit Connection

AIJASET – Vol. 04, No. 02, July 2024. 125-136
https://doi.org/ 10.25077/aijaset.v4i2.136

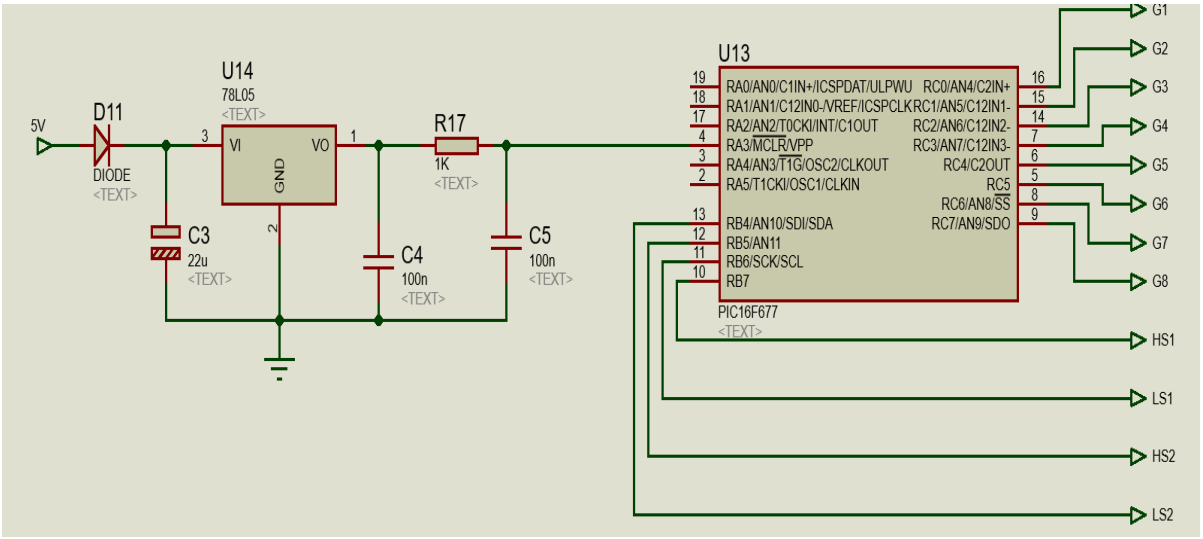

Figure 8. PIC Controller Connection Design

2.11. Simulation Result of the DC-DC Booster

Figure 9 shows the Waveform of DC-DC Converter. The output waveforms confirm that the performance of the inverter design for reality.

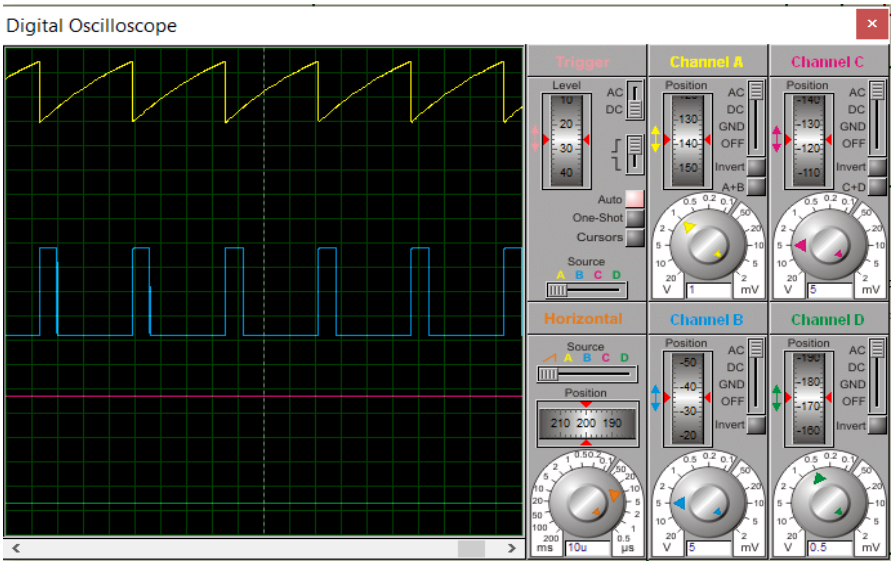

Figure 9. Waveform of DC-DC Converter

2.12. Circuit Diagram of PIC Controller for Simulation

Figure.10 and 11 show the simulation output result of PIC controller used in this system by generating the output wave form using the digital oscilloscope. All of those signals represent each part of the H-bridge inverter respectively. Blue and yellow signals represent the high sides of H-bridge and the remaining twos are for low sides of the inverter. By performing this simulation, whether the PIC program is being written the required.

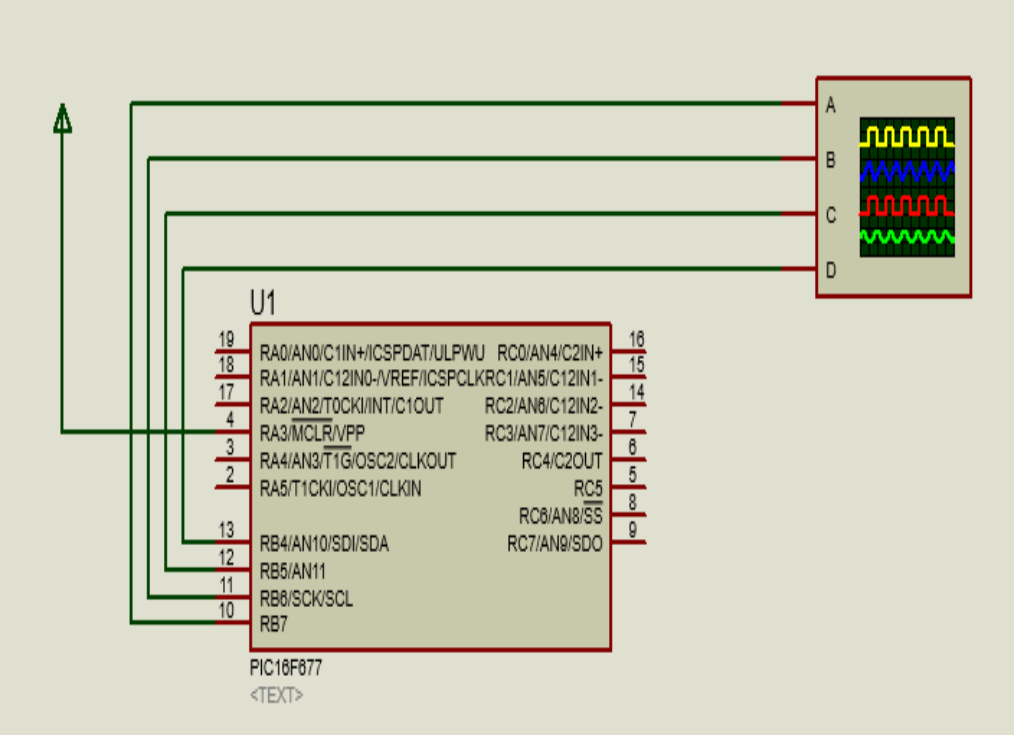

Figure 10. Connection of PIC Controller

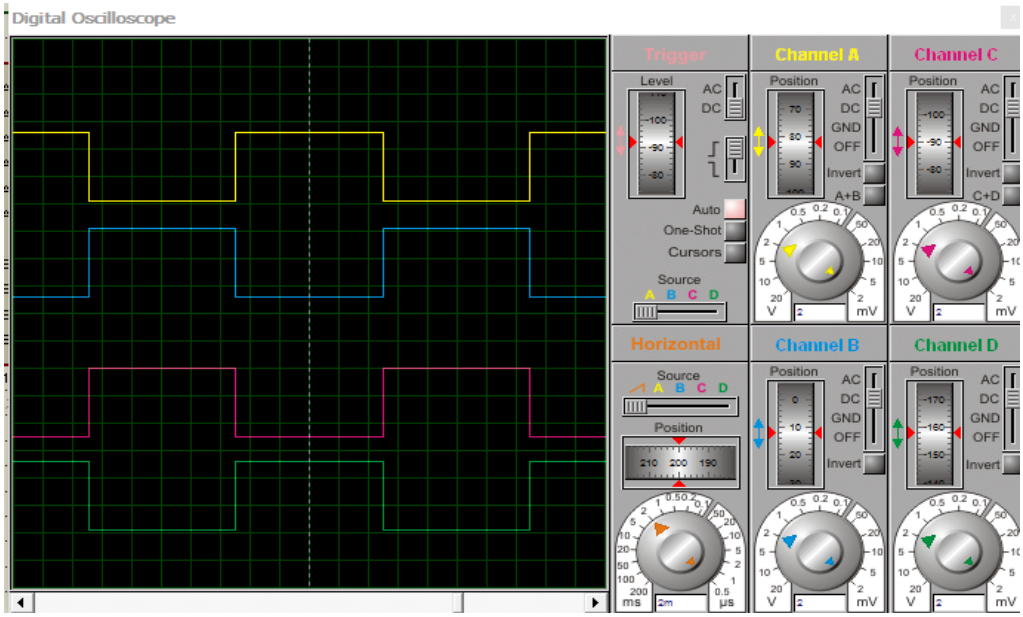

Figure 11. Waveform of PIC Connection with 15 MLI

Figure 12 describes the test and result of the output generated from IRF9540N power MOSFET while figure 1 shows the output waveform. The tests and results of 15-level cascaded H-bridge multilevel converter for variable speed 5kW wind turbine is described. The whole circuit diagram was drawn by using computer-aided software such as Proteus and PCB designer software. The results of hardware testing are described by oscilloscope and measured with digital meter. Figure 14 shows the waveform of the generated AC voltage which has minimum harmonic distortion.

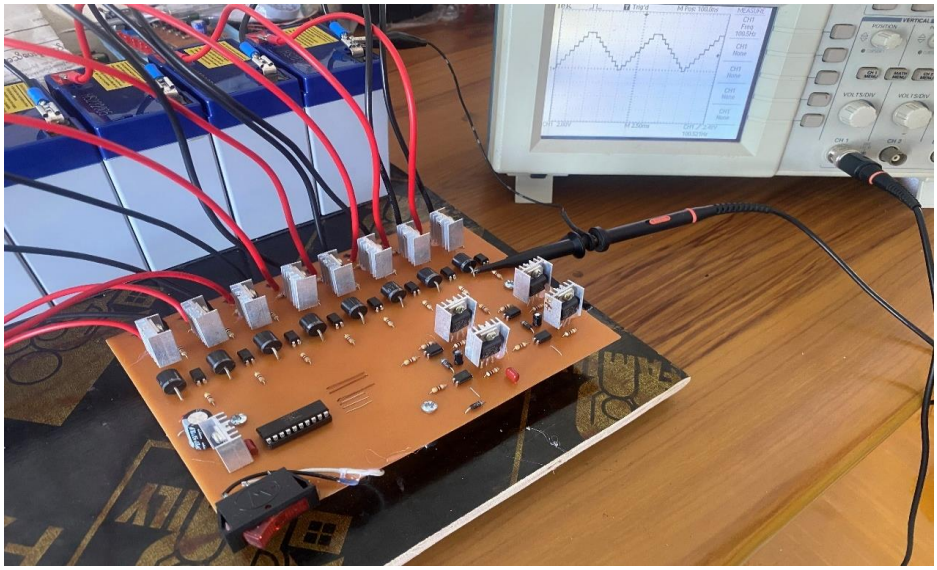

Figure 12. Hardware Testing

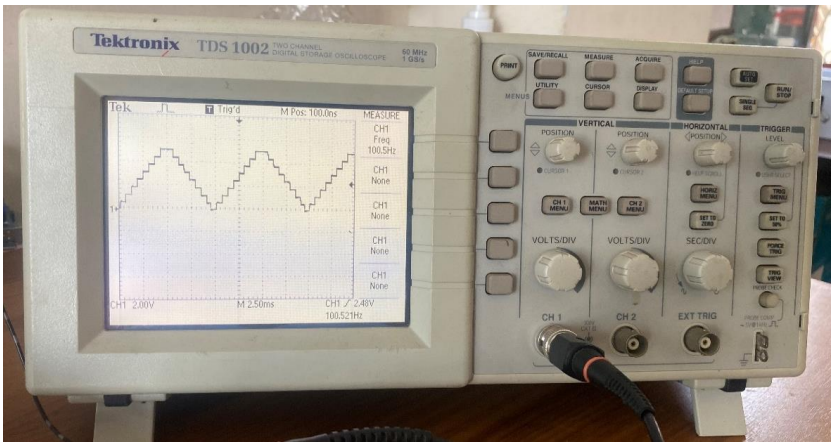

Figure 13. Output Waveform of IRF9540N Power MOSFET

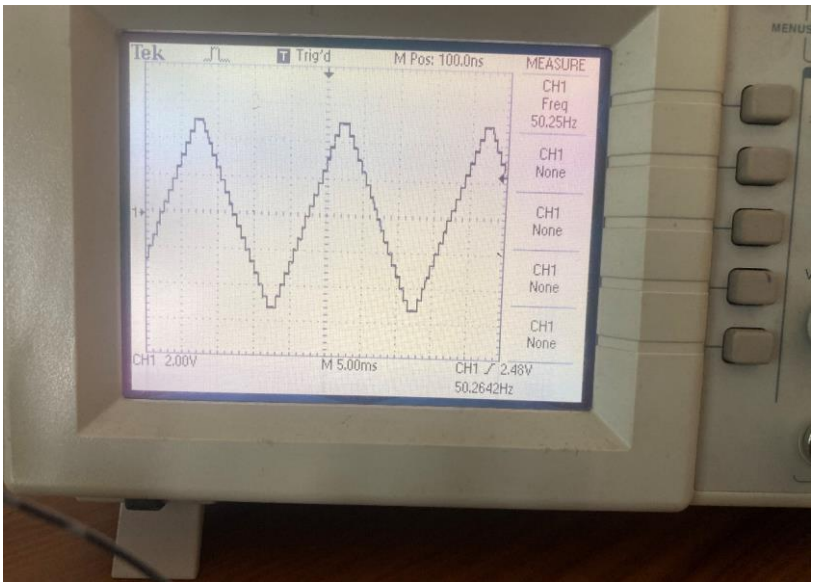

Figure 14. Waveform of Final AC Output Voltage

3. Conclusion

The proposed 15-level cascaded H-bridge multilevel converter is performed as the final important part in the whole wind energy conversion to electricity system because the result is the smoothened and ready-to-use AC voltage for the practical usages. The proposed system is constructed with 6V DC voltage batteries, optocoupler npn, MOSFETs, regulator, PIC controller and other necessary electrical components. The input voltage is obtained from the power source battery bank and then the multilevel MOSFET array and H-bridge inverter, which are controlled by the PIC microcontroller, generated and converted the input DC voltage into the desired output of 15-level steps AC voltage with the minimum harmonic distortion and electromagnetic interference noise. A basic three units will be cascaded and obtained a 15-level MLI configuration was designed. Multilevel converter is of lower harmonics and electromagnetic interference noises. Therefore, multilevel converter is the most promising topology for the grid connection of large wind turbines, especially for offshore wind turbines.

Acknowledgement

The author would like to acknowledge many colleagues from the Electric Vehicles Engineering Research Group under the Department of Electronic Engineering of Yangon Technological University for providing the idea to complete this work. This work is partially supported by Government Research Funds Grant No of GB/D (4)/2019/1.

References

[1] Ahmad Shaharuddin Mat Su,Rasli Abd Ghani,Slamet, Modelling and Simulation of Boost Converter with Maximum Power Point Tracking (MPPT) for Photovoltaic Application, 71:5 (2014) 1–4 | www.jurnalteknologi.utm.my | eISSN 2180–3722 |

[2] A. Anthon, Z. Zhang and M. A. E. Andersen, "Comparison of a state of the art Si IGBT and next generation fast switching devices in a 4 kW boost converter," 2015 IEEE Energy Conversion Congress and Exposition (ECCE), Montreal, QC, Canada, 2015, pp. 3003-3011, doi: 10.1109/ECCE.2015.7310080.

[3] A. A. Saafan, V. Khadkikar, A. Edpuganti, M. S. E. Moursi and H. H. Zeineldin, "A Novel Nonisolated Four-Port Converter for Flexible DC Microgrid Operation," in IEEE Transactions on Industrial Electronics, vol. 71, no. 2, pp. 1653-1664, Feb. 2024, doi: 10.1109/TIE.2023.3257360..

[4] Kunstbergs, N.; Hinz, H.; Schofield, N.; Roll, D. Efficiency Improvement of a Cascaded Buck and Boost Converter for Fuel Cell Hybrid Vehicles with Overlapping Input and Output Voltages. Inventions 2022, 7, 74. https://doi.org/10.3390/inventions7030074.

[5] Dimitrov, B.; Hayatleh, K.; Barker, S.; Collier, G.; Sharkh, S.; Cruden, A. A Buck-Boost Transformerless DC–DC Converter Based on IGBT Modules for Fast Charge of Electric Vehicles. Electronics 2020, 9, 397. https://doi.org/10.3390/electronics9030397.

[6] M. Kumar, R. Bharti and D. V. S. K. Rao K., “Conventional and Hybrid Perturb & Observe based Maximum Power Point Tracking for Solar System,” 2019 International Conference on Vision Towards Emerging Trends in Communication and Networking (ViTECoN), 2019.

[7] Y.-C. Hsieh, T.-C. Hsueh, H.-C. Yen, "An interleaved boost converter with zero-voltage transition", IEEE Trans. Power Electron., vol. 24, no. 4, pp. 973-978, Apr. 2009.

[8] G. R. Walker and P. C. Sernia, “Cascaded DC-DC converter connection of photovoltaic modules,” in IEEE Transactions on Power Electronics, vol. 19, no. 4, pp. 1130-1139, July 2004

[9] EI SHWE ZIN PHYO, KYAW SOE LWIN and HLA MYO TUN, Microcontroller Based Solar Smart Charge Controller using MPPT, vol. 03, no. 06, pp. 0997-1000, May 2014, ISSN 2319-8885.

[10] Tun HM, Aung W (2014) Analysis of control system for A 24 V PM brushed DC motor fitted with an encoder by supplying H-bridge converter. Bahria Univ J Inf Commun Technol 7(1):54–67